HHS Public Access

Author manuscript

Nature. Author manuscript; available in PMC 2013 July 03.

Published in final edited form as:

Nature. 2013 January 3; 493(7430): 106–110. doi:10.1038/nature11693.

Restriction of intestinal stem cell expansion and the regenerative response by YAP

Evan R. Barry[1,2,3], **Teppei Morikawa**[4], **Brian L. Butler**[1,2], **Kriti Shrestha**[1], **Rosemarie de la Rosa**[1], **Kelley S. Yan**[7], **Charles S. Fuchs**[4,8], **Scott T. Magness**[5], **Ron Smits**[9], **Shuji Ogino**[4,6], **Calvin J. Kuo**[7], and **Fernando D. Camargo**[1,2,3,*]

[1]Stem Cell Program and Department of Hematology/ Oncology, Children's Hospital, Boston, MA 02115, USA [2]Department of Stem Cell and Regenerative Biology, Harvard University, Cambridge, MA 02138, USA [3]Harvard Stem Cell Institute, Cambridge, MA 02138, USA [4]Department of Medical Oncology, Dana-Farber Cancer Institute and Harvard Medical School, Boston, MA 02215, USA [5]Departments of Medicine and Biomedical Engineering, The University of North Carolina at Chapel Hill, Chapel Hill, NC 27599, USA [6]Department of Pathology, Brigham and Women's Hospital and Harvard Medical School, Boston, MA 02115, USA [7]Department of Medicine, Hematology Division, Stanford University, Stanford, CA 94305, USA [8]Channing Laboratory, Department of Medicine, Brigham and Women's Hospital and Harvard Medical School, Boston, MA 02115 [9]Department of Gastroenterology and Hepatology, Erasmus MC, 3000 CA Rotterdam, The Netherlands

Abstract

A remarkable feature of regenerative processes is their ability to halt proliferation once an organ's structure has been restored. The Wnt signaling pathway is the major driving force for homeostatic self-renewal and regeneration in the mammalian intestine. The mechanisms that counterbalance Wnt-driven proliferation are poorly understood. We demonstrate here that YAP, a protein known for its powerful growth-inducing and oncogenic properties[1-2], has an unexpected growth-suppressive function restricting Wnt signals during intestinal regeneration. Transgenic expression of YAP reduces Wnt target gene expression and results in the rapid loss of intestinal crypts. In addition, loss of YAP results in Wnt hypersensitivity during regeneration, leading to hyperplasia, expansion of intestinal stem cells (ISCs) and niche cells, and formation of ectopic crypts and microadenomas. We find that cytoplasmic YAP restricts elevated Wnt signaling independently of the APC/Axin/GSK3β complex partly by limiting the activity of Dishevelled (DVL). DVL signals in the nucleus of ISCs and its forced expression leads to enhanced Wnt signaling in crypts. YAP dampens Wnt signals by restricting DVL nuclear translocation during regenerative growth.

*To whom correspondence should be addressed: Fernando.camargo@childrens.harvard.edu.

AUTHOR CONTRIBUTIONS E.R.B. and F.D.C. designed the study. E.R.B, B.L.B., K.S., R.D., and S.T.M. performed experiments. T.M. performed immunohistochemistry and analysis of human tumor samples. K.S.Y., C.S.F., R.S., S.O., and C.J.K. provided reagents for the study.

AUTHOR INFORMATION Microarray data have been deposited in the GEO database under accession number GSE41509.

The authors declare no competing interests.

Finally, we provide evidence that YAP is silenced in a subset of highly aggressive and undifferentiated human colorectal carcinomas (CRC) and its expression can restrict the growth of CRC xenografts. Collectively, our work describes a novel mechanistic paradigm for how proliferative signals are counterbalanced in regenerating tissues. Additionally, our findings have important implications for the targeting of YAP in human malignancies.

YAP is a critical component of the size-controlling Hippo signaling pathway[1-2]. Through a kinase cascade, the pathway targets YAP for phosphorylation, preventing its nuclear translocation where it functions as a transcriptional co-activator. Current dogma suggests that restriction of YAP s transcriptional activity is the principal mechanism of growth and tumor suppression by the Hippo pathway[2]. Indeed, nuclear YAP is a powerful driver of organ growth, progenitor proliferation, and tumor growth[1-4]. We previously assessed YAP function in the mammalian intestine by utilizing a mouse model that resulted in ubiquitous postnatal expression of an inducible YAP-S127A mutant[3]. This mutant protein is thought to have enhanced nuclear localization given that it escapes inactivation by the Hippo kinases LATS1/2[3]. As YAP might activate paracrine signals[5], we sought to bypass non cell-autonomous effects by specifically expressing YAP in the intestinal epithelium using the Villin-rtTA driver [6]. YAP protein in Tg intestine was not restricted to the nucleus, suggesting that S127 is not the major determinant of YAP sub-cellular localization in this tissue (Supplementary Fig 1a). 5-7 days following Dox administration, Tg mice became moribund and were euthanized. Surprisingly, histological evaluation of the small intestine and colon of Tg mice revealed a progressive degenerative phenotype associated with the rapid loss of proliferating crypts (Fig. 1a, Supplementary Fig. 1b, c).

Crypt loss phenotypes are typically associated with reduced Wnt signaling[7]. Indeed, degeneration was accompanied by repression of the Wnt target gene CD44 and loss of cells displaying nuclear β-catenin (Fig. 1b, e and Supplementary Fig. 1e-g). Paneth cells are a mature intestinal lineage that require high levels of Wnt signaling for their proper differentiation and localization, and function as a critical component of the ISC niche [8-9]. In YAP Tg mice, Paneth cells become mislocalized and eventually disappear (Supplementary Fig. 1d). To determine if YAP expression was reducing ISC numbers, we performed *in situ* hybridization (ISH) for *Olfm4*, which marks crypt base columnar (CBCs) stem cells [10]. *Olfm4*+ CBCs were drastically reduced 2 days post induction and were essentially absent by day 4 (Fig. 1c). Consistent with these data, microarray analysis on isolated crypts showed that many of the top downregulated transcripts were known ISC signature genes (i.e.-*Olfm4, Ascl2, Smoc2 and Lgr5*) (Fig. 1d and Supplementary Fig. 2a, b). Gene set enrichment analysis (GSEA) demonstrated significant downregulation of both intestinal β-catenin targets and a recently described ISC gene signature[11,12] (Supplementary Fig. 1c and Supplementary Table 1). Inhibition of growth, loss of Paneth cells and suppression of Wnt/ISC signature genes were confirmed in organoid cultures derived from Tg mice (Supplementary Fig. 1d, e)[9]. Together, these results demonstrate that in contrast to other tissues where it promotes growth, epithelial-specific expression of YAP suppresses intestinal renewal, which occurs through inhibition of the Wnt-signaling pathway.

These observations prompted us to evaluate more carefully the phenotype of gut-specific YAP mutant mice. Consistent with a previous report[13], developmental or acute YAP loss produced no major abnormalities during normal intestinal homeostasis (Fig. 2b and Supplementary Fig. 3a). However, following injury by whole-body irradiation (9 & 11gy), Vill-Cre *Yap* f/f (cKO) mice displayed a striking phenotype of crypt hyperplasia and overgrowth throughout the small intestine and colon (Fig. 2a and Supplementary Fig. 3c, e). This observation contrasts to that of impaired repair observed in a DSS-mediated colitis model[13] (Supplementary Fig. 3b). cKO crypts were hyperproliferative and displayed upregulation of the Wnt target genes CD44 and SOX9 as well as mislocalized and increased numbers of Paneth cells (Fig 2a and Supplementary Fig. 3f). Apoptosis was not altered in cKO mice (Supplementary Fig. 3d). Considering that intestinal regeneration following irradiation is characterized by a state of Wnt hyperactivity[14-15], our data suggest a role for YAP in restricting elevated Wnt signaling *in vivo*.

To directly test if loss of YAP results in Wnt hypersensitivity, we injected adenovirus expressing R-Spondin1 (Ad-RSpo1) into cKO and control mice. RSpo1 is a potent secreted Wnt agonist that induces crypt cell proliferation[16-17]. Seven days after Ad-RSpo1 injection, 80% of cKO mice (n=8) became moribund and were euthanized, whereas Ad-Fc injected control mice (n=8) appeared normal. cKO intestines and colon displayed a massively hyperplastic phenotype so that by day 7, most mature intestinal lineages in cKO epithelia were replaced by highly proliferative crypt-like tissue (Fig. 2b,c and Supplementary Fig. 4a-i). Hyperplasia was accompanied by upregulation of Wnt targets CD44, SOX9 and EPHB3, in addition to global upregulation of the intestinal β-catenin target signature (Fig. 2d-f and Supplementary Fig. 4j). To determine if YAP loss resulted in expansion of cells with the features of ISCs, we generated cKO:*Lgr5-EGFP* mice. LGR5 is normally expressed in the CBCs at the very bottom of the crypt (Fig. 2g inset), however, following RSpo1 administration in control mice, the population of *Lgr5+* ISCs is expanded (Fig. 2g). This expansion is much more striking in the cKO intestine, where the *Lgr5+* domain is 3-4 times in size. ISC expansion was confirmed by ISH for *Olfm4*, and GSEA (Supplementary Fig. 5a and Fig. 2e and Supplementary Table 1). cKO mice also displayed a dramatic increase in Paneth cell numbers (Fig. 2h and Supplementary Fig. 5b, c and d). Paneth cells and Lgr5+ cells were evident high in the crypt/villus axis (Fig. 2g, Supplementary Fig. 5d). cKO mice also displayed ectopic epithelial foci resembling crypts formed within villi that stained positive for CD44, Lys, and proliferative markers (Fig. 2i and Supplementary Fig. 5e-g). Some of these progressed into structures reminiscent of microadenomas, precancerous lesions where outpocketing pouches of crypt-like tissue grow into normal villi (Supplementary Fig. 5g). These were never observed in control RSpo1-treated animals. Together, these results demonstrate that YAP restricts the expansion of ISCs as well as critical components of the stem cell niche.

To gain insight into the mechanism behind our observations, we revisited the expression pattern of YAP in the intestine. It has previously been shown that YAP protein is primarily localized to the crypt base, and is absent from villi[3,13]. Using a new polyclonal antibody, we find that YAP is nuclear enriched in CBCs and lower crypt cells (Supplementary Fig. 6a-c) but also expressed in upper TA (transit amplifying) cells and throughout the villi, where it is

predominantly cytoplasmic (Supplementary Fig. 6a). This was confirmed by cellular fractionation experiments (Supplementary Fig. 6d). YAP localization correlated to the staining pattern of CD44, demonstrating that nuclear YAP is present in zones of active Wnt signaling, but is mostly cytoplasmic where Wnt is restricted (Supplementary Fig. 6e). These data suggest that cytoplasmic YAP might be functionally responsible to terminate Wnt signaling and allow progress from a proliferative progenitor/stem cell compartment to a postmitotic, differentiated fate. To rule out the possibility that a transcriptional function of YAP was repressing Wnt, we generated *Yap*$^{fl/S79A}$ *Villin-Cre* mice. The YAP protein in these mutants cannot bind to TEAD transcription factors, the main transcriptional effectors of YAP [18-19]. Following RSpo1 injection, we observed no enhanced Wnt response in YAP S79A mutant mice (Supplementary Fig. 7a). Supporting a role for cytoplasmic YAP in restricting Wnt signaling, expression of YAP-WT and a YAP-S127D phospho-mimic limited Wnt reporter responsiveness in 293T cells (Supplementary Fig. 7b, c).

The phenotype observed in cKO mice treated with RSpo1 histologically resembled acute *Apc* deletion (Supplementary Fig. 8)[20]. Surprisingly, we observed no obvious changes in β-catenin protein levels in hyperplastic cKO crypts (Supplementary Fig. 8a-c). As increases in β-catenin protein are the direct consequence of disrupting the AXIN/APC/GSK3β complex, these data suggest that YAP restriction of Wnt signaling is likely not mediated by modulating the activity of this complex. It has been recently suggested that phosphorylated YAP (cytoplasmic) sequesters β-catenin in the cytoplasm in cell lines[21]. Though we observed a subtle expansion in the number of nuclear β-catenin positive cells in cKO mucosa (Supplementary Fig. 8b), these likely represent the expansion of Paneth cells and we infer that this does not represent the major mechanism of YAP-mediated Wnt repression. In vitro, we observed increased Wnt activity after combined YAP and APC depletion versus APC only knockdown, and a synergistic effect of YAP depletion together with GSK3β small molecule inhibition (Supplementary Fig. 8d, e). In mice, combined deletion of APC and YAP (DKO) versus APC only in an acute or a long-term adenoma model[22] resulted in a robust upregulation of CD44 in addition to significant increases in the number of Paneth cells and proliferative cells (Supplementary Fig. 9a-g). Thus, our data suggest that YAP acts to restrict Wnt signaling independently, and in some cases synergistically, to the activity of destruction complex and control of subcellular localization of β-catenin.

Recently, it was reported that TAZ, a protein that bears a 57% homology to YAP, interacts with Dishevelled (DVL)[23], a positive Wnt signaling regulator. Work primarily done in *Drosophila* has shown that DVLs act in the cytoplasm upstream of the β-catenindestruction complex. However, emerging work in mammals suggest that DVL also exists in the nucleus mediating the Wnt transcriptional response partly in conjunction with c-Jun and TCF4 [24-25]. We determined that YAP also interacts with DVL2 (Supplementary Fig. 10a). The function of DVLs in intestinal regeneration has been poorly characterized, although the observation that loss of DVL2 causes a decrease in intestine length and crypt diameter suggests an important role in intestinal biology[26]. We find that DVL2 expression is restricted to the crypt compartment, where it is localized in the nucleus of CBCs and assumes a more diffuse pattern in the TA compartment (Fig. 3a). Furthermore, DVL2 nuclear localization is enhanced in crypts after RSpo1 administration and during regeneration following irradiation

(Fig. 3b and Supplementary Fig. 10b). To evaluate the role of nuclear DVL in crypts, we infected organoids with lentiviruses expressing a Dox-inducible DVL carrying a nuclear localization signal (DVL-NLS)[25]. DVL-NLS increases Wnt target gene expression and leads to the transient formation of spheroid organoids resembling those with constitutive Wnt signaling (Fig. 3e)[9]. In addition, expression of DVL-NLS after APC knockdown results in a synergistic activation of the TOPflash Wnt reporter (Supplementary Fig. 10c). Thus, our findings are consistent with an important nuclear function of DVL in intestinal progenitors and Wnt signaling in parallel or downstream to the destruction complex.

Given the observed physical interaction between YAP and DVL2 and their overlapping patterns of sub-cellular localization in crypts, we hypothesized that YAP might control DVL2 sub-cellular localization and/or activity. We observed a massive expansion of cells positive for nuclear DVL2 in cKO mice treated with RSpo1 and during radiation-induced regeneration (Fig. 3b and Supplementary Fig. 10b). Additionally, YAP knockdown led to DVL nuclear accumulation in DLD1 cells (Fig. 3c and Supplementary Fig. 10d,e). We found no increase in levels of nuclear β-catenin in this context (Supplementary Fig. 10e). Loss of DVL2 and DVL3 partially or completely rescued increased Wnt target genes in the absence of YAP (Fig. 3d). To determine if YAP could block DVL-induced Wnt transcriptional responses, we generated organoids expressing Dox-inducible DVL-NLS (Supplementary Fig. 10f) and YAP. Expression of YAP completely abrogated the DVL-mediated upregulation of the Wnt target genes *Lgr5 and Axin2* (Fig. 3e). Therefore, we conclude that YAP is critical for the proper sub-cellular localization of DVLs and blocks their ability to induce Wnt signaling.

Lastly, we investigated the role of YAP in human CRC. Using DLD1 cells infected with Dox inducible YAP-WT or YAP-S127D, we performed xenograft assays to assess the effect of YAP on tumor growth. We found a dramatic decrease in tumor growth with the addition of Dox, particularly with YAP-S127D (Fig. 4a and Supplementary Fig. 11a, b). This decrease in tumor size coincided with global suppression of the CRC TCF4/β-catenin[27] and ISC[11] gene signatures (Fig. 4b, c, Supplementary Fig. 11c, d and Supplementary Table 1). We next examined if YAP loss was associated with human CRC by evaluating YAP expression in a cohort of 672 CRC samples using immunohistochemistry[28]. Complete loss of YAP staining occurred within a minor subset of human tumors (10.5%), but predicted worse patient survival and was associated with high grade, stage IV disease, compared to YAP positive groups (Supplementary Fig. 11e-h and Fig. 4d-f). These results are consistent with our animal data and demonstrate that YAP may act as a tumor suppressor in human CRC.

Precise mechanisms must exist to dampen proliferative potential to maintain organ size. Here, we have identified YAP and DVLs as key players in this process by restricting the expansion of ISCs and their niche during Wnt-driven regeneration. Although we have not ruled out a pro-proliferative role for nuclear YAP, our results suggest that the predominant function of YAP in the intestine is growth-restrictive. During normal development and homeostasis, TAZ (whose expression is highly enriched in crypts - Supplementary Fig. 6d) might be compensating for the loss of YAP. Alternatively, YAP together with DVL might be part of a regeneration-exclusive molecular machinery that helps counteract hyperactive

Wnt signaling, which occurs during emergency growth. Interestingly, YAP is a WNT target gene[29], suggesting that it might participate in a negative feedback loop to limit WNT-initiated signals. Current therapeutic efforts are aimed at diminishing YAP protein levels in many malignancies, including CRC[30]. Our results suggest that such manipulations could potentially result in increased tumor growth. YAP targeting therapies should aim to disrupt the YAP/TEAD interaction or induce the cytoplasmic translocation of YAP. Further study of the role of YAP as a growth suppressor is likely to provide important insight into the biology of regeneration, size control, and tumor progression.

METHODS

Mice

Yap1 conditional knockout and *S79A* point mutant mice were previously described [19]. *Yap1* cKO mice were intercrossed with *Villin-Cre*[31] , *Villin-CreER* [32], *Lgr5-EGFP-IRES-CreER* [33], and *Apc fl/fl* mice [34]. Mice were given a single dose of tamoxifen (1mg in corn oil injected i.p.) in *Yap/Apc* conditional knockout experiments with *Villin-CreER*. *Villin-rtTA* mice were described previously [6].

For *in vivo* administration of R-Spondin1, adenovirus expressing Fc-tagged R-Spondin1 of mouse origin was retro-orbitally injected at 3×10^8 PFU. Virus was produced as previously described [16]. Tissue was collected at 3.5 or 7 days. For irradiation experiments, mice were exposed to 9 or 11Gy at a dose of 0.664Gy/minute from Cesium 137-irradiator. Tissue was collected 5 days after irradiation.

Immunohistochemistry of mouse tissue

Staining was performed with the following antibodies using the Vectastain ABC-Elite kit according to manufacturers instructions, with the exception of Cryptdin1, which was detected using an anti-goat Alexa-Fluor 488 (Invitrogen): rabbit anti-YAP (Cell Signaling 1:40, Avruch Lab 1:400), mouse anti-PCNA (Santa Cruz Biotechnology), rat anti-CD44 (BD Biosciences 1:100), rat anti-Ki67 (Dako 1:40), rabbit anti-phospho histone H3 (Millipore 1:300), rabbit anti-SOX9 (Millipore 1:300), goat anti-EPHB3 (R&D 1:300), rabbit anti-GFP (Abcam 1:3000), goat anti-Cryptdin1 (Andre Ouellette), rabbit anti-DVL2 (Cell Signaling 1:100). Antigen retrieval was performed using low pH citrate buffer. Staining for β-Catenin was performed as previously described[35]. Lysozyme staining was performed as follows (Dako Rabbit anti-Human Lysozyme). Antigen retrieval was performed by proteinase-K digestion at 37 degrees for exactly 12 minutes in tris-EDTA pH 9 followed by PBS wash for 5 minutes and quenching of endogenous peroxidases and Vectastain ABC-Elite kit processing. Next, tissue was incubated in primary antibody at 1:1000 in PBS 0.1% Triton at 4 degrees overnight.

In situ hybridization

In situ hybridization for *Olfm4* transcripts was performed on formalin fixed intestine at the specialized histopathology service core at the Dana Farber Cancer Institute using RNAscope, according to manufacturer's instructions.

Quantification of H3S10ph and Lysozyme foci

For Villin-CreER experiments, lysozyme quantification was performed on a cohort of five control (*Apc fl/fl*) and 5 double cKO (*Yap1 fl/fl Apc fl/fl*) mice. The quantification was performed blind to specimen identity. Paneth cell numbers were quantified by the number of crypt cells staining positive for lysozyme on a per-crypt basis. For each sample, per-crypt numbers of Lysozyme positive cells were averaged over at least fifteen 10× fields of view per mouse. In Villin-CreSt experiments, H3S10ph and Lysozyme positivity was counted in a similar manner. Student's *t-test* was used to determine statistical significance with a cutoff of $P<0.05$.

DSS treatment

Mice were given 2.5% DSS in drinking water for 7 days, followed by normal drinking water for 3 days. Colon tissue was snap frozen and cryosections were stained with hematoxylin to visualize tissue architecture.

siRNA mediated knockdown

Cells were reverse transfected with 7nM final concentration of indicated siRNA (Ambion Silencer Select) using Lipofectamine RNAiMax (Invitrogen), according to manufacturer's instructions. For expression analysis in DLD1 cells, RNA was extracted 4 days after transfection. Oligos against human transcripts used were (5′-3′): *siAPC* Sense: *GGAUCUGUAUCAAGCCGUUtt*, Antisense: *AACGGCUUGAUACAGAUCCtt* (ol i g o # s1433), *siYAP* Sense: *GGUGAUACUAUCAACCAAAtt*, Antisense: *UUUGGUUGAUGUAUCACCtg* (oligo # s20366), *siDVL3* Sense: *GAUAUGUUGUUACAGGUAAtt*, Antisense: *UUACCUGUAACAACAUAUCtc* (oligo # s675), *siDVL2* (pooled 2 siRNAs) Sense: *CACCAUCCCUAAUGCCUUUtt*, Antisense: *AAAGGCAUUAGGGAUGGUGat* (oligo # s4396) and Sense: CAGUCACGCUAAACAUGGAtt, Antisense: UCCAUGUUUAGCGUGACUGtg (Oligo # s4398).

RNA extraction, cDNA synthesis and quantitative PCR

RNA was extracted from cells or tissue using RNeasy mini kit according to manufacturer's instructions (Qiagen). cDNA synthesis was performed on 1ug of total RNA using iScript cDNA synthesis kit (Biorad). QPCR was performed using Taqman probes available from Applied Biosystems and Taqman Fast-Advanced master mix. Probed used were as follows: mouse *Cd44* Mm01277163_m1, *Lgr5* Mm00438890_m1, *Myc* Mm004877804, *Wwtr1* (*Taz*) Mm00513560_m1, *Nkd1* Mm00471902_m1, *Yap* Mm00494240_m1, *Sox9* Mm00448840_m1, *Cd133 (Prom1)* Mm00477115_m1, *Axin2* Mm00443610_m1, *Apc* Mm00545877_m1 and *Fabp2* Mm00433188_m1. Human probes were: *NKD1* Hs00263894_m1 and *FOXN1* Hs00263894_m1. All reactions were run on Applied Biosystems Step-One-Plus real-time PCR instrument and data were calculated using the delta-delta Ct method. Significance values were calculated using Student's t-Test with a P value cutoff of less than 0.05.

Immunofluorescence

For immunocytochemistry of adherent DLD1 cells, cultures were grown on sterile coverslips and washed once with PBS followed by fixation in 4% paraformaldehyde/PBS for 15 minutes at room temperature. Cells were then washed twice with cold PBS and permeabilized with PBS/0.25% Triton X-100 for 10 minutes at room temperature. Cells were then washed three times in PBS followed by blocking in 1% BSA/PBS for 30 minutes at room temperature. Next, cells were incubated in primary antibodies in 1% BSA/PBS overnight at 4 degrees followed by 3 washes in PBS. Cells were then incubated for 1 hour in dark humidified chamber with Alexa-fluor conjugated secondary antibodies in 1% BSA/PBS followed by 3 washes in PBS. Coverslips were then stained with DAPI and mounted on glass slides. Staining was performed with the following antibodies: Mouse anti-YAP (Santa Cruz 1:500) and rabbit anti-DVL2 (Millipore 1:200).

Co-immunoprecipitation

293T cells were transiently transfected with GFP (negative control) or indicated flag-tagged versions of YAP2 (Plasmids purchased from Addgene, originally constructed in the lab of Marius Sudol) or myc-tagged DVL2 (from the Xi He lab) using Lipofectamine 2000. After 48 hours, cells were lysed in buffer containing 1% Triton X-100, 50mM Tris HCl pH 7.4, 150mM NaCl and 1mM EDTA followed by passage through 26 gauge needle 10 times. Lysates were precleared with protein-A agarose and then incubated in anti-Flag resin (Sigma Aldrich) for 1 hour 30 minutes while shaking. Protein complexes were then washed 4 times in lysis buffer and boiled for western detection. Mouse anti-Flag M2 antibody (Sigma Aldrich) was used at 1:1000 to detect flag-tagged YAP and rabbit anti-Myc antibody (Sigma Aldrich 1:1000) was used to detect myc-tagged DVL2.

Subcellular fractionation

DLD1 cells were reverse transfected with indicated siRNA. After 4 days, cells were washed with PBS, scraped and centrifuged. Cells were then resuspended in 3-4 pellet volumes of fractionation buffer containing sucrose, HEPES, KCl, MgCl, EDTA, NP-40, protease and phosphatase inhibitors. Cells were then passed through a 25 ½ gauge needle 10 times and left on ice for 20 minutes and then centrifuged to pellet nuclei away from cytoplasm. Nuclei were then washed by passage through 25 ½ gauge needle 10 times and centrifuged. Nuclear and cytoplasmic fractions were then resuspended in equal volumes of lysis buffer and analyzed by Western blots. The following antibodies were used: mouse anti-YAP (Santa Cruz 1:1000), rabbit anti-DVL2 (Cell Signaling 1:1000), anti-Fibrillarin (Abcam 1:1000), anti-Beta Tubulin (Cell Signaling 1:1000).

Wnt reporter assays

293T cells were first transfected with the indicated siRNA. Two days later, TOPflash and Renilla plasmids were cotransfected. Wnt activity was assayed 48 hours after reporter transfection. All values are represented as the ratio of firefly to renilla. Transfections were performed in triplicate.

A stable 293T cell line was used in BIO and Wnt3A + RSpo1 induction experiments. This line was created by co-transfecting the TOPflash plasmid with a renilla expressing plasmid

(10:1 ratio of firefly to renilla) carrying a blasticidin resistance selection marker. Cells were selected under 6ug/ml. Clones were picked, expanded and screened for TOPflash activity after treatment with recombinant Wnt3A. YAP and scrambled siRNAs were transfected at 7nM, and induced with Wnt3A and Wnt3A (500ng/ml) +RSpondin1 (500ng/ml) 3 days later when cells were approximately 50% confluent, for 16hrs. Induction with bromoindirubin (5uM) (BIO Sigma Aldrich) was performed in the same manner as with Wnt3A and RSpo1. Controls were treated with DMSO. To test the effect of nuclear localized DVL in 293T WNT reporter assays, a DVL-NLS expressing construct [25] was transiently transfected with renilla and TOPflash plasmids 3 days after siRNA treatment. Luciferase levels were measured 48 hours later.

Microarray Analysis

In Tg experiments, whole RNA was extracted from mouse crypts. RNA was extracted from whole epithelium in RSpo1 experiments. Microarray experiments were performed by the Microarray Core of the Molecular Genetics Core Facility at Children's Hospital Boston. Material was processed for Affymetrix Mouse GeneChip 1.0ST arrays. For each experimental condition, 3 mice were used. CEL files were converted to GCT files using ExpressionFileCreator in Gene Pattern, publicly available from the Broad Institute (genepattern.broadinstitute.org). GCT files were preprocessed and used in the Comparative Marker Selection module to obtain lists of differentially regulated genes. In Tg experiments, a threshold of p<=0.05 and fold change of 1.4 or greater was used. In RSpo1 experiments, fold change of 2 and q-value (FDR corrected p-value) of 0.05 were used as cutoffs. Expression analysis of human xenograft tumors was performed using Affymetrix Human GeneChip 1.0ST chips and processed as above. GCT files were used in Comparative Marker Selection. RNA was used from 3 control (no dox) and 3 YAP-S127D dox induced tumors. Threshold cutoffs were p<=0.05 and fold change of 1.4-fold or greater. Gene Set Enrichment Analysis was performed using GCT files from Yap experiments compared to gene sets cited in the main text.

Organoid culture and lentiviral infection

Organoids were derived, propagated and infected according to previously published work [36-37]. pINDUCER20[38] was used for inducible lentiviral expression studies in DLD1 xenografts and organoids.

Human colorectal cancer clinical sample analysis Study population

The databases of two nationwide prospective cohort studies were utilized: the Nurses' Health Study (N=121,701 women followed since 1976) and the Health Professionals Follow-up Study (N=51,529 men followed since 1986) [28]. We collected paraffin-embedded tissue blocks from hospitals throughout the U.S. where patients underwent colorectal cancer resections. Hematoxylin and eosin stained tissue sections from all colorectal cancer cases were reviewed by a pathologist (S.O.) unaware of other data. Tumor grade was categorized as low vs. high (>50% vs. ≤50% gland formation). We excluded cases which were preoperatively treated. Patients were observed until death or January 1, 2011, whichever came first. Death of a participant was confirmed by the National Death Index. Returning questionnaire indicated informed consent from all study participants. This study was

approved by the Human Subjects Committees at Harvard School of Public Health and Brigham and Women's Hospital.

Immunohistochemistry on human samples

Tissue microarrays were constructed as previously described 39. For YAP immunohistochemistry, deparaffinized tissue sections were treated with Antigen Retrieval Citra Solution (Biogenex Laboratories, San Ramon, CA) in microwave for 15 min. Tissue sections were then incubated with Peroxidase Blocking Reagent (15 min; DAKO) and primary antibody against YAP (rabbit polyclonal, 1:400 dilution; Cell Signaling) was applied, and slides were incubated for 16 h at 4 degrees. Next, we applied SignalStain® Boost IHC Detection Reagent (Cell Signaling) for 30 min followed by visualizing signal with diaminobenzidine (5 min; DAKO) and hematoxylin counterstain. Each immunohistochemical maker was evaluated by a pathologist (T.M.) unaware of other data.

Statistical analysis

All statistical analyses were performed by SAS program (Version 9.1, SAS Institute, Cary, NC). All p values were two-sided and statistical significance was set at p=0.05. For categorical data, the chi-square test was performed. Kaplan-Meier method and log-rank test were used for survival analyses.

Supplementary Material

Refer to Web version on PubMed Central for supplementary material.

ACKNOWLEDGEMENTS

We thank Len Zon and Camargo lab members for critical review of this manuscript and Xi He for Myc-DVL2 constructs. This work was supported by grants from the Stand Up to Cancer-AACR initiative (FDC), NIH R01 CA131426 and AR064036 (FDC), and the Harvard Stem Cell Institute (FDC). FDC is a Pew Scholar in the Biomedical Sciences. EB is supported by a postdoctoral fellowship from the American Cancer Society Illinois Division (PF-12-245-01-CCG). Other support includes KSY (CIRM, and 1K08DK096048), CJK (1U01DK085527), SO (R01 CA151993), and CSF (P50CA127003).

References

1. Pan D. The hippo signaling pathway in development and cancer. Dev Cell. 2010; 19:491–505. [PubMed: 20951342]
2. Ramos A, Camargo FD. The Hippo signaling pathway and stem cell biology. Trends Cell Biol. 2012; 22:339–46. [PubMed: 22658639]
3. Camargo FD, et al. YAP1 increases organ size and expands undifferentiated progenitor cells. Curr Biol. 2007; 17:2054–60. [PubMed: 17980593]
4. Dong J, et al. Elucidation of a universal size-control mechanism in Drosophila and mammals. Cell. 2007; 130:1120–33. [PubMed: 17889654]
5. Zhang J, et al. YAP-dependent induction of amphiregulin identifies a non-cell-autonomous component of the Hippo pathway. Nat Cell Biol. 2009; 11:1444–50. [PubMed: 19935651]
6. Roth S, et al. Generation of a tightly regulated doxycycline-inducible model for studying mouse intestinal biology. Genesis. 2009; 47:7–13. [PubMed: 18942097]
7. Pinto D, Gregorieff A, Begthel H, Clevers H. Canonical Wnt signals are essential for homeostasis of the intestinal epithelium. Genes Dev. 2003; 17:1709–13. [PubMed: 12865297]

8. Andreu P, et al. A genetic study of the role of the Wnt/beta-catenin signalling in Paneth cell differentiation. Dev Biol. 2008; 324:288–96. [PubMed: 18948094]
9. Sato T, et al. Paneth cells constitute the niche for Lgr5 stem cells in intestinal crypts. Nature. 2011; 469:415–8. [PubMed: 21113151]
10. van der Flier LG, et al. Transcription factor achaete scute-like 2 controls intestinal stem cell fate. Cell. 2009; 136:903–12. [PubMed: 19269367]
11. Munoz J, et al. The Lgr5 intestinal stem cell signature: robust expression of proposed quiescent '+4' cell markers. EMBO J. 2012; 31:3079–91. [PubMed: 22692129]
12. Fevr T, Robine S, Louvard D, Huelsken J. Wnt/beta-catenin is essential for intestinal homeostasis and maintenance of intestinal stem cells. Mol Cell Biol. 2007; 27:7551–9. [PubMed: 17785439]
13. Cai J, et al. The Hippo signaling pathway restricts the oncogenic potential of an intestinal regeneration program. Genes Dev. 2010; 24:2383–8. [PubMed: 21041407]
14. Ashton GH, et al. Focal adhesion kinase is required for intestinal regeneration and tumorigenesis downstream of Wnt/c-Myc signaling. Dev Cell. 2010; 19:259–69. [PubMed: 20708588]
15. Davies PS, Dismuke AD, Powell AE, Carroll KH, Wong MH. Wnt-reporter expression pattern in the mouse intestine during homeostasis. BMC Gastroenterol. 2008; 8:57. [PubMed: 19055726]
16. Ootani A, et al. Sustained in vitro intestinal epithelial culture within a Wnt-dependent stem cell niche. Nat Med. 2009; 15:701–6. [PubMed: 19398967]
17. Kim KA, et al. Mitogenic influence of human R-spondin1 on the intestinal epithelium. Science. 2005; 309:1256–9. [PubMed: 16109882]
18. Zhao B, et al. TEAD mediates YAP-dependent gene induction and growth control. Genes Dev. 2008; 22:1962–71. [PubMed: 18579750]
19. Schlegelmilch K, et al. Yap1 acts downstream of alpha-catenin to control epidermal proliferation. Cell. 2011; 144:782–95. [PubMed: 21376238]
20. Sansom OJ, et al. Loss of Apc in vivo immediately perturbs Wnt signaling, differentiation, and migration. Genes Dev. 2004; 18:1385–90. [PubMed: 15198980]
21. Imajo M, Miyatake K, Iimura A, Miyamoto A, Nishida E. A molecular mechanism that links Hippo signalling to the inhibition of Wnt/beta-catenin signalling. EMBO J. 2012; 31:1109–22. [PubMed: 22234184]
22. Cheung AF, et al. Complete deletion of Apc results in severe polyposis in mice. Oncogene. 2010; 29:1857–64. [PubMed: 20010873]
23. Varelas X, et al. The Hippo pathway regulates Wnt/beta-catenin signaling. Dev Cell. 2010; 18:579–91. [PubMed: 20412773]
24. Itoh K, Brott BK, Bae GU, Ratcliffe MJ, Sokol SY. Nuclear localization is required for Dishevelled function in Wnt/beta-catenin signaling. J Biol. 2005; 4:3. [PubMed: 15720724]
25. Gan XQ, et al. Nuclear Dvl, c-Jun, beta-catenin, and TCF form a complex leading to stabilization of beta-catenin-TCF interaction. J Cell Biol. 2008; 180:1087–100. [PubMed: 18347071]
26. Metcalfe C, et al. Dvl2 promotes intestinal length and neoplasia in the ApcMin mouse model for colorectal cancer. Cancer Res. 2010; 70:6629–38. [PubMed: 20663899]
27. Van der Flier LG, et al. The Intestinal Wnt/TCF Signature. Gastroenterology. 2007; 132:628–32. [PubMed: 17320548]
28. Chan AT, Ogino S, Fuchs CS. Aspirin and the risk of colorectal cancer in relation to the expression of COX-2. N Engl J Med. 2007; 356:2131–42. [PubMed: 17522398]
29. Konsavage WJ, Kyler SL, Rennoll SA, Jin G, Yochum GS. Wnt/b-catenin signaling regulates Yes-associated protein (YAP) gene expression in colorectal carcinoma cells. J Biol Chem. 2012; 287:11730–9. [PubMed: 22337891]
30. Avruch J, Zhou D, Bardeesy N. YAP oncogene overexpression supercharges colon cancer proliferation. Cell Cycle. 2012; 11:1090–6. [PubMed: 22356765]
31. Madison BB, et al. Cis elements of the villin gene control expression in restricted domains of the vertical (crypt) and horizontal (duodenum, cecum) axes of the intestine. J Biol Chem. 2002; 277:33275–83. [PubMed: 12065599]
32. el Marjou F, et al. Tissue-specific and inducible Cre-mediated recombination in the gut epithelium. Genesis. 2004; 39:186–93. [PubMed: 15282745]

33. Barker N, et al. Identification of stem cells in small intestine and colon by marker gene Lgr5. Nature. 2007; 449:1003–7. [PubMed: 17934449]
34. Colnot S, et al. Colorectal cancers in a new mouse model of familial adenomatous polyposis: influence of genetic and environmental modifiers. Lab Invest. 2004; 84:1619–30. [PubMed: 15502862]
35. Barker N, et al. Crypt stem cells as the cells-of-origin of intestinal cancer. Nature. 2009; 457:608–11. [PubMed: 19092804]
36. Koo BK, et al. Controlled gene expression in primary Lgr5 organoid cultures. Nat Methods. 2012; 9:81–3. [PubMed: 22138822]
37. Sato T, et al. Single Lgr5 stem cells build crypt-villus structures in vitro without a mesenchymal niche. Nature. 2009; 459:262–5. [PubMed: 19329995]
38. Meerbrey KL, et al. The pINDUCER lentiviral toolkit for inducible RNA interference in vitro and in vivo. Proc Natl Acad Sci U S A. 2011; 108:3665–70. [PubMed: 21307310]
39. Ogino S, et al. Combined analysis of COX-2 and p53 expressions reveals synergistic inverse correlations with microsatellite instability and CpG island methylator phenotype in colorectal cancer. Neoplasia. 2006; 8:458–64. [PubMed: 16820091]

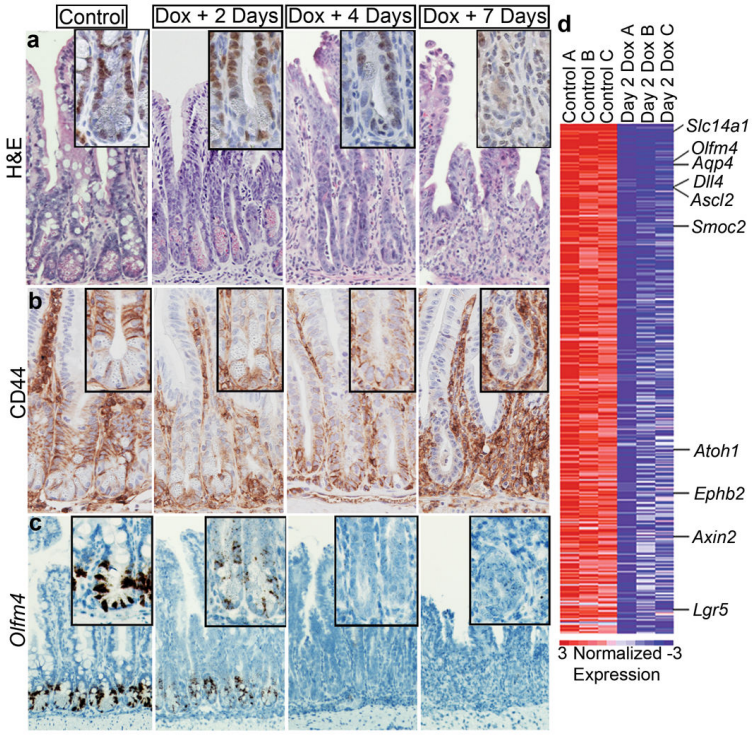

Figure 1. YAP overabundance inhibits Wnt-mediated intestinal regeneration

a, H&E staining of doxycycline induced YAP-S127A small intestine at 2, 4 and 7 days. Inset of Ki67 stain representative of crypt proliferation. **b, c,** Wnt pathway activity and ISC presence at 2, 4 and 7 days post dox induction represented by CD44 **(b) and** *Olfm4* (*in-situ*) **(c). d,** Heatmap of crypts isolated from control (n=3) and day 2 dox (n=3) treated mice displaying 540 downregulated genes in rank order. Labeled genes are examples known to be involved in Wnt signaling and the ISC niche. Original magnifications in each panel are 20x (**a, b**), 10x (**c**).

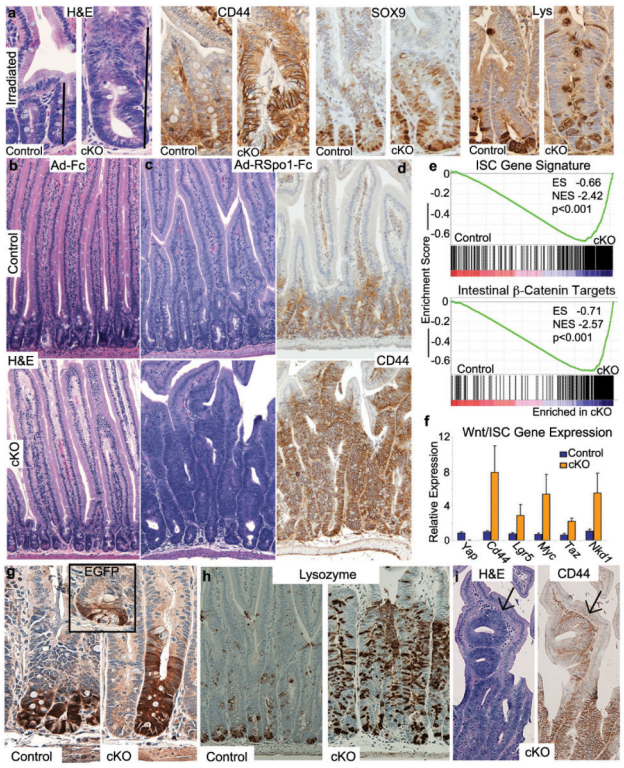

Figure 2. Loss of YAP leads to hyperactive Wnt signaling and expansion of the stem cell niche after injury or stimulation with RSpo1

a, H&E, CD44, SOX9 and Lysozyme staining of small intestinal crypts in control and cKO mice 1 week after irradiation. **b,** H&E of inert virus treated control and cKO small intestine. **c, d,** H&E staining **(c)** and CD44 IHC **(d)** in control and cKO mice 1 week after administration of adenovirus expressing RSpo1. **e**, GSEA of the ISC gene signature and intestine-specific β-catenin target gene sets. Black bars represent individual genes in rank order. **f**, Q-PCR validating several upregulated Wnt/ISC markers. **g, h,** IHC on small intestine of control and cKO small intestine for EGFP (expressed from the Lgr5 locus, inset is an untreated mouse) **(g)** and Lysozyme marking Paneth cells **(h)**. **i,** Ectopic crypt formation in cKO mice treated with RSpo1 stained for H&E or the Wnt target CD44. Original magnifications in each panel are 20x (**a**), 10x (**b-d**), 20x (g) and 10x (**h, i**). Graphed data represent the mean and S.E.M. of 3 individual mice per genotype.

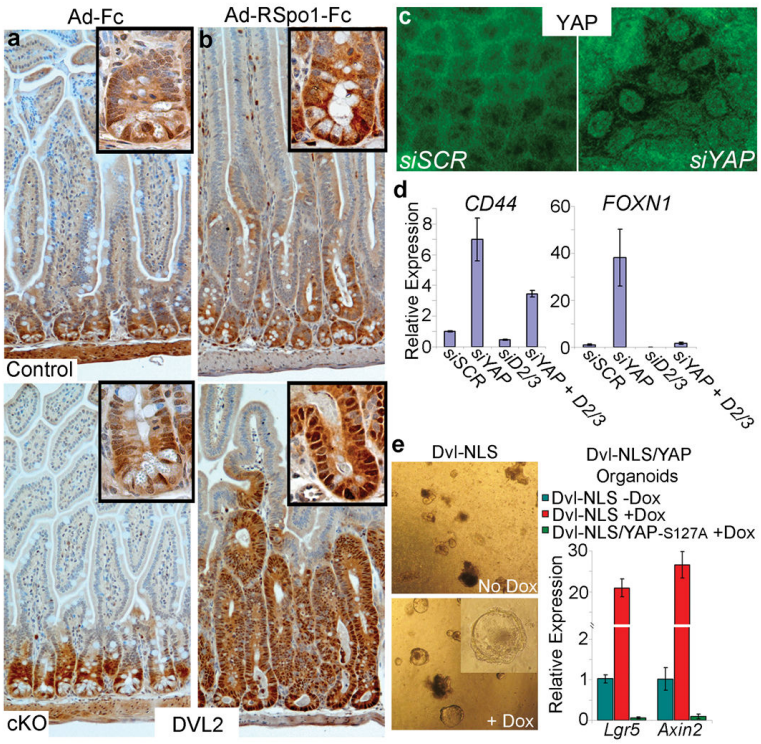

Figure 3. YAP restricts Wnt signaling by blocking DVL nuclear translocation

a, b, DVL2 IHC in control and cKO small intestine treated with Ad-Fc **(a)** and Ad-RSpo1-Fc **(b)**. Insets are higher magnifications showing subcellular localization of DVL2. **c,** Immunofluorescent staining for DVL2 in confluent DLD1 cells after transfection with indicated siRNA. **d,** Expression analysis of Wnt target genes in DLD1 cells after transfection with siRNAs against YAP, DVL2+DVL3 (D2/3) or YAP + D2/3. **e,** Expression analysis of organoids infected with lentivirus encoding Dox-inducible DVL-NLS alone, or in a Villin-rtTA TetO-YAP-S127A background. Dox was given in culture medium for 4 days. All graphed data represent the mean and standard deviation of triplicate cultures.

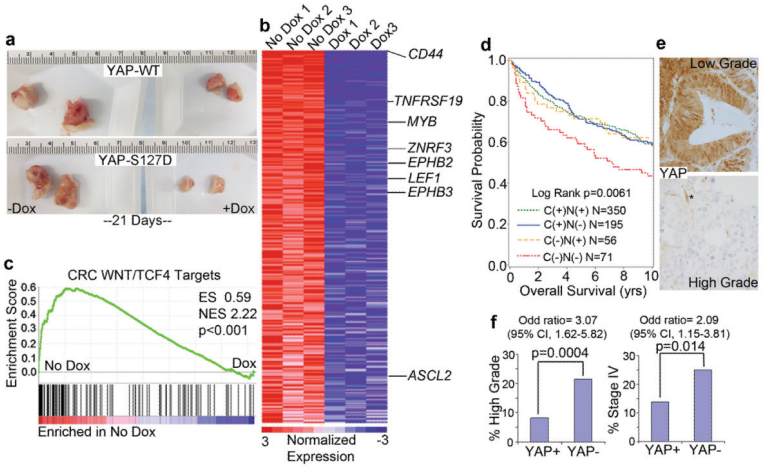

Figure 4. YAP function in human colorectal cancer

a, Xenograft tumor formation of DLD1 cells infected with lentivirus encoding Dox-inducible YAP-WT or YAP-S127D mutant. Tumor photos are representative images. **b,** Heatmap representing the top 328 genes downregulated by YAP-S127D induction in xenograft assays (n=3 tumors per treatment group). Labeled genes are known β-catenin targets in human CRC. **c**, GSEA of TCF4-dependent CRC target genes. **d,** Overall survival analysis of patients with specific YAP staining patterns. YAP IHC was placed into 4 groups of staining patterns correlating with subcellular localization from 672 colorectal cancer patients: Cytoplasmic and nuclear (C (+) N (+)), Cytoplasmic (C (+) N (−)), Nuclear positive (C (−) N (+)) and Complete loss of staining (C (−) N (−)). **e,** YAP staining in low and high grade tumors. **f,** YAP loss is significantly associated with high grade tumors and stage IV disease (CI, confidence interval).